Wetlands
https://doi.org/10.1007/s13157-018-1104-8

ORIGINAL RESEARCH

Carbon Storage in Secondary Mangroves along the West Coastline of Maputo City, Mozambique

Tarquinio Mateus Magalhães [1]

Received: 5 June 2017 / Accepted: 29 October 2018

Abstract

Mangroves are often excluded when estimating carbon (C) from global and tropical forests. Therefore, C estimates of global and tropical forests are likely to be underestimated. On the other hand, allometric biomass models and C stocks estimates are lacking for juvenile mangrove trees (seedling and sapling), yet required for increasing of young successional mangrove forests as result of disturbances. In this study, allometric biomass models were fitted and ecosystem C stock estimated for a juvenile secondary mangrove forest, using a non-destructive biomass sampling. Besides the advantage of enforcing additivity and being least biased, the models fitted simultaneously using nonlinear seemingly unrelated regression (NSUR) with parameter restriction were superior with regard to predictive accuracy and ability compared to those fitted independently. The surface soil accounted for the majority of the ecosystem C stock (90%). Aboveground biomass ranked next with 9.6% of the ecosystem C stock.

Keywords *Avicennia marina* · Biomass · Carbon stocks · Necromass · Non-destructive sampling · Soil organic carbon

Introduction

Mangroves are salt tolerant plants that grow within the intertidal region between the sea and the land along tropical and subtropical coasts. They are known to protect coastlines from wave energy and protect offshore ecosystems from terrestrial sediments flowing downstream (Taylor et al. 2003). They provide habitat for over 1300 animal species and are one of the most productive ecosystems (Fatoyinbo et al. 2008).

Mangroves are often excluded when estimating carbon (C) stocks and carbon dioxide (CO_2) emissions from global and tropical forests (e.g. Pan et al. 2011; Baccini et al. 2012; Ladd et al. 2012; Zarin 2012). Therefore, C estimates of global and tropical forests are likely to be underestimated. Recent studies (e.g. Donato et al. 2011; Jachowski et al. 2013; Hamilton and Lovette 2015) have shown that mangrove forest C storage per unit area is approximately three to four times higher than that of other tropical forests including rainforests, implying that the deforestation of mangrove forests releases more CO_2 per unit area than other global forest types.

The global area of mangrove forests is estimated to be 14 Mha, distributed in 118 countries and territories in the tropical and subtropical regions of the world (Geri et al. 2011). About ¾ of world's mangroves are found in just 15 countries (Geri et al. 2011). Mozambique is among the 15 most mangrove-rich countries with 2.3% (318,851 ha) of world's mangroves area (Geri et al. 2011). In Africa, Mozambique has the second largest area of mangrove, with 12% of the continent's mangrove area (FAO 2007).

At global level, mangrove forests are most at risk of conversion to aquaculture, while non-mangrove tropical forests are often converted to agriculture (Hamilton and Lovette 2015). In Mozambique, where the coastal population is about 2/3 of the total population (Hoguane 2007), the overall deforestation rate of mangroves is estimated at 2.6% (Barbosa et al. 2001; Taylor et al. 2003), and considered to be relatively unaffected (Taylor et al. 2003) compared to other countries. However, Maputo and Beira cities (the two largest cities of Mozambique) have experienced much mangrove deforestation for firewood, charcoal, agriculture, salt production (Taylor et al. 2003), and most importantly, urban sprawl, thus having a higher rate of deforestation (Barbosa et al. 2001).

✉ Tarquinio Mateus Magalhães
tarqmag@yahoo.com.br

[1] Departamento de Engenharia Florestal, Universidade Eduardo Mondlane, Campus Universitário, Edificio no. 1, 257, Maputo, Moçambique

Published online: 07 November 2018

Mangroves of the west coastline of Maputo city have been extremely devastated due to urban sprawl and other anthropogenic uses such as firewood collection. To avoid total devastation, the study area was set as a protected area by the municipality of Maputo. The area is mainly composed by seedlings and sampling of *Avicennia marina* (Forssk.) Vierh. with a relative abundance >95% (Amade 2006).

Biomass models and estimates for juvenile trees (seedling and sapling) are scarce in the literature (Annighöfer et al. 2016), as most published biomass models focus on larger trees (DBH ≥ 10 cm). Yet, biomass estimates for seedlings and saplings are required for increasing of young successional forests as result of disturbances (Annighöfer et al. 2016) and to model their future development and predict the dynamics in C cycling of forests (Galik et al. 2009).

On the other hand, woody debris are an important forest ecosystem component as they provide information on quality and status of wildlife habitats, structural diversity within the forest, C sequestration, storage and cycling of nutrients and water (Harmon et al. 1986; Husch et al. 2003). Wood debris are also very important for seedling establishment, soil development, provision of habitat for decomposers and heterotrophs and are a source of energy and nutrients (Harmon and Hua 1991). Yet, they are a neglected component of terrestrial and aquatic ecosystems (Harmon et al. 1986) and a neglected C pool (Chao et al. 2008; Merganičová and Merganič 2010).

The objective of this study was to fit allometric biomass models for each tree component and estimate the C stored in biomass, necromass and in the soil of a secondary Mangrove forest along the west coastline of Maputo city, in Mozambique, southern Africa.

Material and Methods

Study Area

The study area (Fig. 1) is bounded by the meridians 32°37′30″ and 32°39′05″ eastern longitudes and parallels 25°54′15″ and 25°55′45″southern latitudes in the west coastline of Maputo city, Mozambique, occupying about 139 ha, and it is located less than 250 m from sea.

The altitude of the study area varies from 1 to 8 m above the mean sea level; the climate is humid tropical (DINAGECA 1997). According to the United Nations Food and Agriculture Organization (FAO) classification (FAO 2003), the soils of the study area are Salic Fluvisols. The mean annual temperature of Maputo city is approximately 23° C with a mean annual minimum temperature of approximately 18° C and a mean annual maximum temperatures ranging from 28 to 29 ° C (CMM 2010). The mean annual precipitation ranges from 633 to 916 mm (CMM 2010).

Data Acquisition and Analysis

Live Aboveground Biomass

Two-phase sampling design was used to estimate biomass and carbon stocks. In the first phase, seventy two (72) 0.04 ha (20 m × 20 m) random sampling plots were allocated in the study area, comprising a sampling intensity of 2.1%. Within the plots all trees with root collar diameter (RCD) ≥ 1 cm were measured for RCD, tree height (H), live crown length (LCL), and crown radius and consequently crown diameter (CD). Refer to Table 1 for summary statistics of the phase-1 data. RCD was preferred over diameter at breast height (DBH) because a considerable number of trees in the study area has not achieved the breast height. RCD was measured using a caliper or a caliper rule and the heights were measured using a telescopic measuring pole or a ruler. Crown radius was measured using a right-angle prism densiometer and a tape, from the centre of the trunk to the perimeter of the crown, in four cardinal directions (North, South, East and West). CD was computed as double of the geometric mean crown radius.

In the second phase, 2 to 6 trees representing all RCD classes and all species found within each plot were selected for non-destructive biomass measurement. Non-destructive biomass measurement was preferred over destructive one because the study area is protected by the municipality of Maputo. The stem was divided into 5 segments equal in length and the diameter of each segment was measured at the midpoint. Length and three diameter measurements (on the bottom, middle and top) were taken in each primary, secondary and higher-order branch. The upper diameters and branches of the tallest trees were measured with the aid of a step ladder.

The thickest primary branch was cut down from each phase-2 tree using a pruning shear or a chainsaw and a basal wood section of approximately 10–15 cm in length was collected from the branch. The wood sections were dipped in drums filled with water, until constant weight, for its saturation and subsequent determination of the saturated volume and basic density. Saturated volume was obtained based on the water displacement method (Brasil et al. 1994). Wood sections were oven dried at 105 °C to constant weight. Basic density was obtained by dividing the oven-dry mass by the relevant saturated volume (de Gier 1992; Bunster 2006).

Stem and branch volumes were computed using Hohenadl's and Newton formulae, respectively (Husch et al. 2003; Magalhães and Seifert 2015), and their dry masses were calculated by multiplying the volumes by the basic wood density.

To estimate the foliage dry mass, additional to the cut branch, 2 to 4 primary branches representing all size classes were selected and their leaves collected. The foliage of each branch was oven-dried at 105 °C until their constant mass, hereafter the dry mass measured. The foliage dry

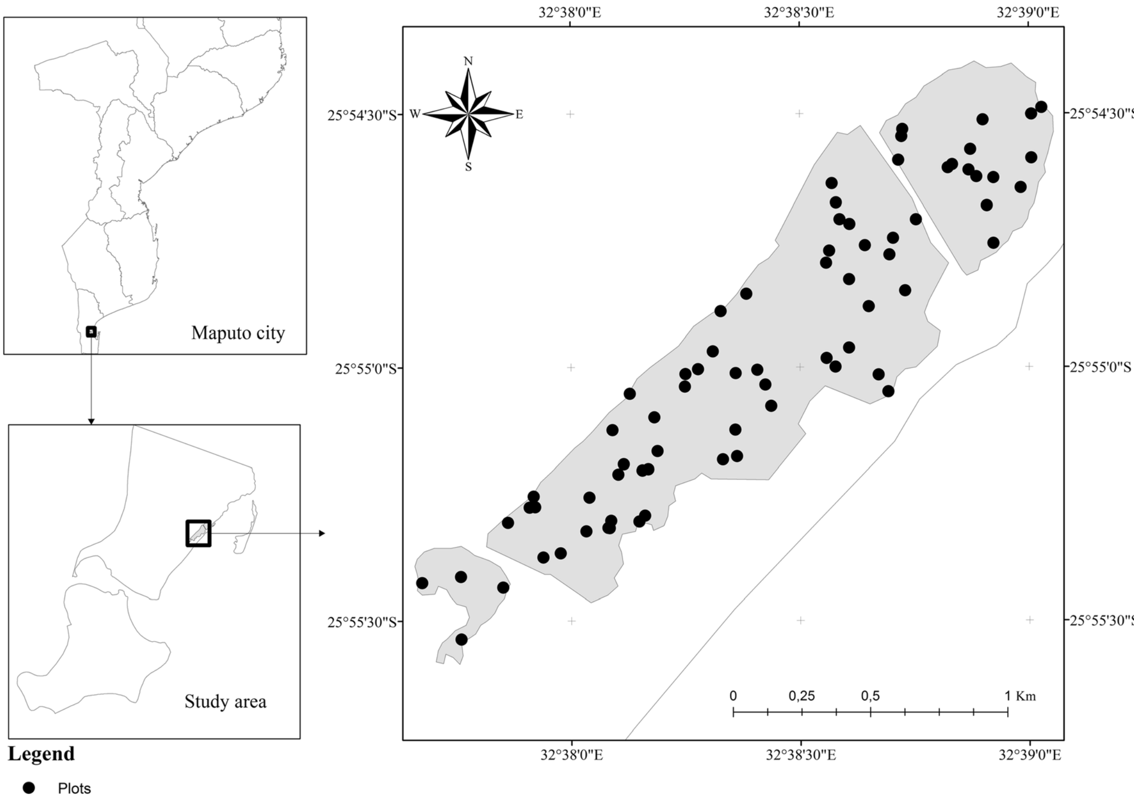

Fig. 1 Distribution of sampling plots in the study area

mass was up-scaled from the branch level to the tree level by multiplying the weighted mean foliage dry mass per branch (weighted by branch volume) by the total number of primary branches of the tree.

The following tree biomass components were considered: (1) stem, (2) branches, (3) foliage, (4) crown (2 + 3), and (5) shoot system (1 + 4). Biomass models were fitted separately for each tree biomass component. No species-specific models were fitted because the study area is mainly composed by *Avicennia marina* (Forssk.) Vierh. with a relative abundance >95%. The summary statistics of the phase-2 data are provided in Table 2. The phase-2 data (301 trees) were split in training (227) and testing data (74), for model fitting and validation, respectively.

Because biomass is a nonlinear function of the independent variables (Ter-Mikaelian and Korzukhin 1997; Schroeder et al. 1997; Bolte et al. 2004; de Jong and Klinkhamer 2005; Salis et al. 2006), the models were fitted using nonlinear least squares.

The following models were tested for all tree biomass components

$$Y = \alpha RCD^{\beta} + \varepsilon \tag{1}$$

$$Y = \alpha RCD^{\beta} H^{\gamma} + \varepsilon \tag{2}$$

Additionally, the models below were also tested for foliage, branches, crown and AGB

$$Y = \alpha RCD^{\beta} LCL^{\gamma} + \varepsilon \tag{3}$$

$$Y = \alpha RCD^{\beta} CD^{\gamma} + \varepsilon \tag{4}$$

where Y is aboveground or tree component biomass [Kg]; α, β and γ are regression parameters and ε is the error term.

Models were fitted using the nls function of R software (R Core Team 2016) and evaluated based on the following goodness-of-fit statistics: Akaike information criterion (AIC; Akaike 1973), mean residuals (MR [%]), coefficient of variation of residuals (CV_r [%]), Furnival's index of fit (FI; Furnival 1961), and model prediction error (MPE). MPE

Table 1 Summary basic statistics of phase-1 data

Statistic	RCD [cm]	H [m]	CD [m]	LCL [m]
Minimum	1.00	0.20	0.26	0.05
Maximum	24.00	9.80	3.49	9.30
Average	6.63	1.35	0.83	0.68
SD	3.62	0.90	0.35	0.76
CV	54.64	66.51	42.48	111.59
SE	0.11	0.03	0.01	0.02
SE [%]	1.68	2.05	1.31	3.43
n	1056	1056	1056	1056

SD standard deviation, *SE* standard error, *CV* coefficient of variation, *n* sample size

Table 2 Summary basic statistics of phase-2 data

	Variables	Minimum	Maximum	Average	SD	CV [%]	SE	SE [%]	n
Dendrometric variables	RCD [cm]	1.00	16.00	6.43	3.39	52.75	0.23	3.50	301
	H [m]	0.30	7.00	1.41	1.08	76.31	0.07	5.07	301
	CD [m]	0.27	3.18	0.88	0.44	50.32	0.03	3.34	301
	LCL [m]	0.10	6.25	0.80	0.97	120.91	0.06	8.03	301
Dry mass [kg]	Stem	4E – 03	106.15	11.74	18.96	161.54	1.23	10.72	301
	Foliage	3E – 03	16.67	2.31	3.34	144.28	0.22	9.58	301
	Branches	0.12	44.66	7.66	7.22	94.15	0.48	6.25	301
	Crown	0.12	58.41	9.98	10.35	103.75	0.69	6.89	301
	Shoot system	0.13	156.66	21.72	28.85	132.84	1.92	8.82	301

was estimated for each model by K–fold cross-validation (K = 10) using cvFit function from the package "cvTools" (Alfons 2015) of R software (R Core Team 2016). Models resulting in least and not significant MR, smallest AIC, CVr, FI, and MPE were selected as the best.

Coefficient of determination (R^2) was not used to evaluate the performance of the models because it is inappropriate when used for demonstrating the performance or validity of nonlinear models (Spiess and Neumeyer 2010). This is because the regression sum-of-squares and the residual sum-of-squares do not add up to total sum-of-squares as in linear least squares, and thus R^2 is no longer between 0 and 100%.

The biomass predictions from the minor tree component models (e.g. foliage, branches, and stem) will not sum to those from the major tree component models (e.g. crown, and shoot system), not achieving biomass additivity, which is illogical. To enforce additivity, new major component model forms were obtained as a function of the predictors of the best minor component models. The new major component model forms and the best minor component model forms were fitted again, simultaneously, using nonlinear seemingly unrelated regression (NSUR) with parameter restriction. NSUR with parameter restriction is the most statistically sound method of enforcing the property of additivity for nonlinear biomass models (Parresol 2001).

The simultaneous models (NSUR models) were fitted using PROC MODEL statement of SAS software (SAS Institute Inc. 1999), using the ITSUR option. Restrictions on the regression coefficients were imposed by using RESTRICT statement. The NSUR models were applied to phase-I data to estimate plot and stand level biomass.

The biases resulting from the independently and simultaneously fitted models were determined by Eq. 5 using the testing data.

$$\mathrm{Bias} = \frac{\sum PB_k - \sum OB_k}{\sum PB_k} \times 100\% \qquad (5)$$

where PB_k and OB_k represent the predicted and observed biomass, respectively, of the c component of the k^{th} tree. The biases were tested for significance using Wilcoxon signed rank test. Further, Pearson's correlation coefficient was used to evaluate the degree of which the predicted biomass is associated with observed biomass. All the analyses were performed at 5% significance level.

All living stumps within the main plot were measured for volume similarly to branches, and a disc removed on top of it for the determination of basic density and dry mass as done for branches. The dry mass of the stumps was obtained by multiplying the volume of the stumps by mean basic density of the sample stumps.

C stored in biomass was obtained as half of the dry mass (IPCC 2003; Elias and Potvin 2003).

Necromass

In the North corner of each plot, a 5 m × 5 m subplot was established for measurement of coarse woody debris (CWD), defined here as the woody material ≥2.0 cm in diameter at the wider end, regardless of the length. Fine wood debris (FWD, woody material <2.0 cm in diameter at the wider end) and litter were observed in a 1 m × 1 m quadrat established in the North corner of the subplots. CWD were divided into standing and fallen. Standing CWD comprised snags (standing dead trees) and dead stumps. Fallen CWD comprised logs (fallen dead trees), their attached and detached branches and other woody parts detached from the tree that can be classified as coarse.

Snags and dead stumps were measured for dry mass similarly to standing live trees and living stumps, respectively. Fallen CWD were measured for fresh mass in the field and a sample of 5–10% of the fresh mass (representing all size classes) was taken to the laboratory for oven-drying at 105 °C until constant mass. The dry mass of the fallen CWD of each subplot was obtained by multiplying the ratio of oven-dry- to fresh-mass of the sample by the relevant total fresh mass. FWD + litter were measured similarly to fallen CWD. The dry masses of standing and fallen CWD were up-scaled to per unit area measurements using the expansion factor [i.e. the ratio of unit area (ha) to the subplot or quadrat area]. C stored in necromass was obtained as half of the dry mass (IPCC 2003; Elias and Potvin 2003).

Soil

Soil samples, disturbed and undisturbed, were collected within the 1 m × 1 m quadrats. Disturbed soil samples for estimation of soil organic matter (SOM) content and soil organic carbon (SOC) content [%] were collected using a Dutch auger of 30 cm depth. Therefore, soils were assessed to 30 cm depth from the ground level (0–30 cm soil layer), following the minimum depth recommended by IPCC (2006). After removing the litter, disturbed soil samples were collected at each corner of each quadrat. A homogenized subsample of the 4 samples was taken to the laboratory for SOC and SOM content determination using the Walkley-Black method (Pearson et al. 2005).

Soil samples for estimation of bulk density (undisturbed soil cores) were collected in the centre of the quadrats using a 100 cm^3 volume corer (height: 51 mm, inner diameter: 50 mm). For each point (plot centre), undisturbed soils cores were taken from three soil layers within the major layer (0–30 cm): superficial layer (0–10 cm), intermediate layer (10–20 cm), and deep layer (20–30 cm). Bulk density was calculated for every soil sample as the ratio of oven-dry soil mass to the volume of the corer.

The SOC stock of the population was computed using Eq. 6 (Pearson et al. 2005; Zhou et al. 2007)

$$\mathrm{SOC_{Stock}} = \mathrm{D} \times \overline{\mathrm{B}} \times \overline{\mathrm{O}} \quad \left[\mathrm{Mg\ ha^{-1}}\right] \tag{6}$$

where D is the soil depth interval [cm]; $\overline{B}$ and $\overline{O}$ are the mean soil bulk density [g cm^{-3}] and the mean SOC content [%].

Results

The RCD of the phase-1 trees varied from 1 to 24 cm, while that of phase-2 trees varied from 1 to 16 cm. Tree height (H) varied from 0.2 to 9.8 m for phase-1 trees, and from 0.3 to 7.0 m for phase-2 (Tables 1 and 2). However, phase-1 trees with RCD > 16 cm represented only 2% of the sampled trees; and only 2 trees of the phase-1 were out of phase-2 height range. Of the 1056 trees sampled during the phase-1 only 8 were from *Rhizophora mucronata* species, the rest were from *Avicennia marina*. All of the phase-2 trees (331) were from *Avicennia marina* species. Therefore, the phase-2 data were representative of the phase-1 data.

Tables 3 and 4 give the regression parameters, and goodness-of-fit statistics for the tested models, respectively. The predictor H was not statistically significant for estimating stem, and branches biomasses, and LCL and CD were not significant for estimating foliage biomass (Table 3); the inclusion of those predictors resulted in higher AIC and MPE values (Table 4). But then, the inclusion of H and CD in foliage and branches biomass models, respectively, resulted in significantly lower AIC, FI, CVr values (i.e. improved predictive accuracy) and negligible changes in MPE (i.e. no significant changes in predictive ability). Improved predictive accuracy and ability was also observed for the crown and AGB models when CD was included as a predictor.

Equation 1 ($\hat{Y} = \alpha \mathrm{RCD}^{\beta}$), Eq. 2 ($\hat{Y} = \alpha \mathrm{RCD}^{\beta}\mathrm{H}^{\gamma}$), and Eq. 4 ($\hat{Y} = \alpha \mathrm{RCD}^{\beta}\mathrm{CD}^{\gamma}$) were selected as the best allometric biomass models for stem, foliage, and branches, respectively, based mainly on AIC, FI, and CVr, as MRs were not found to be statistically different from zero (Table 4) and MPE did not differ significantly between models tested for same tree components.

Equation 4 ($\hat{Y} = \alpha \mathrm{RCD}^{\beta}\mathrm{CD}^{\gamma}$) was also elected the best for crown and AGB. However, as mentioned previously, the biomass estimates from stem, foliage, and branches models will not sum to that of AGB model. Similarly, the biomass estimates from foliage, and branches models will not sum to that of crown model. This compromises the property of additivity.

To achieve additivity, a new crown biomass model form was set up as a function of the predictors of the best foliage, and branches model forms; and a new AGB model form was also set up as a function of the predictors of the best stem, and the new crown model forms. The new model forms (crown and AGB) along with the previous selected model forms (stem, foliage, and branches) were fitted again, simultaneously, using NSUR with parameter restriction. The structural system of model forms (to be fitted simultaneously) is given in Eq. 7.

$$\begin{aligned}
\hat{Y}_{\mathrm{Stem}} &= \alpha_1 \mathrm{RCD}^{\beta_1} \\
\hat{Y}_{\mathrm{Foliage}} &= \alpha_2 \mathrm{RCD}^{\beta_2}\mathrm{H}^{\gamma_2} \\
\hat{Y}_{\mathrm{Branches}} &= \alpha_3 \mathrm{RCD}^{\beta_3}\mathrm{CD}^{\gamma_3} \\
\hat{Y}_{\mathrm{Crown}} &= \alpha_2 \mathrm{RCD}^{\beta_2}\mathrm{H}^{\gamma_2} + \alpha_3 \mathrm{RCD}^{\beta_3}\mathrm{CD}^{\gamma_3} \\
\hat{Y}_{\mathrm{AGB}} &= \alpha_1 \mathrm{RCD}^{\beta_1} + \alpha_2 \mathrm{RCD}^{\beta_2}\mathrm{H}^{\gamma_2} + \alpha_3 \mathrm{RCD}^{\beta_3}\mathrm{CD}^{\gamma_3}
\end{aligned} \tag{7}$$

where $\hat{Y}_{\mathrm{Crown}}$ and $\hat{Y}_{\mathrm{AGB}}$ are restricted to have the same predictors and regression parameters as the constituent component models.

All the regression parameters of the simultaneously fitted models were statistically significant (Table 5). By using the NSUR approach, the predictive accuracy and ability of the crown biomass and AGB models improved significantly (Table 6) when compared to the previously selected independent models: for the crown biomass model, AIC, FI, CVr, and MPE had a decline of about 2, 7, 11, and 29%, respectively. On the other hand, a decline of approximately 1, 6, 10, and 22% was observed for AGB model, respectively. A slight but non-significant increase in AIC, FI, CVr, and MPE was observed for the minor tree components models (stem, foliage, branches) when fitted simultaneously.

Table 3 Regression parameters of independently fitted allometric biomass models

Tree component	Model form	α (± SE)	β (± SE)	γ (± SE)
Stem	$\hat{Y} = \alpha RCD^{\beta}$	0.03 (± 0.01)	2.86 (± 0.09)	–
	$\hat{Y} = \alpha RCD^{\beta}H^{\gamma}$	0.03 (± 0.01)	2.88 (± 0.11)	– 0.01 (± 0.06)^{ns}
Foliage	$\hat{Y} = \alpha RCD^{\beta}$	0.01 (± 3E – 03)	2.55 (± 0.09)	–
	$\hat{Y} = \alpha RCD^{\beta}H^{\gamma}$	0.02 (± 4E – 03)	2.42 (± 0.11)	0.14 (± 0.06)
	$Y = \alpha RCD^{\beta}LCL^{\gamma}$	0.01 (± 4E – 03)	2.51 (± 0.10)	0.03 (± 0.04)^{ns}
	$\hat{Y} = \alpha RCD^{\beta}CD^{\gamma}$	0.02 (± 4E – 03)	2.49 (± 0.10)	0.07 (± 0.05)^{ns}
Branches	$\hat{Y} = \alpha RCD^{\beta}$	0.39 (± 0.07)	1.55 (± 0.08)	–
	$\hat{Y} = \alpha RCD^{\beta}H^{\gamma}$	0.45 (± 0.09)	1.46 (± 0.10)	0.09 (± 0.07)^{ns}
	$\hat{Y} = \alpha RCD^{\beta}LCL^{\gamma}$	0.50 (± 0.10)	1.44 (± 0.08)	0.11 (± 0.04)
	$\hat{Y} = \alpha RCD^{\beta}CD^{\gamma}$	0.64 (± 0.13)	1.32 (± 0.09)	0.29 (± 0.06)
Crown	$\hat{Y} = \alpha RCD^{\beta}$	0.29 (± 0.05)	1.81 (± 0.08)	–
	$\hat{Y} = \alpha RCD^{\beta}H^{\gamma}$	0.34 (± 0.07)	1.71 (± 0.10)	0.11 (± 0.06)
	$\hat{Y} = \alpha RCD^{\beta}LCL^{\gamma}$	0.37 (± 0.08)	1.70 (± 0.09)	0.10 (± 0.04)
	$\hat{Y} = \alpha RCD^{\beta}CD^{\gamma}$	0.44 (± 0.09)	1.61 (± 0.09)	0.23 (± 0.06)
Shoot system	$\hat{Y} = \alpha RCD^{\beta}$	0.16 (± 0.03)	2.44 (± 0.08)	–
	$\hat{Y} = \alpha RCD^{\beta}H^{\gamma}$	0.17 (± 0.04)	2.38 (± 0.10)	0.05 (± 0.06)^{ns}
	$\hat{Y} = \alpha RCD^{\beta}LCL^{\gamma}$	0.16 (± 0.04)	2.43 (± 0.09)	0.01 (± 0.03)^{ns}
	$\hat{Y} = \alpha RCD^{\beta}CD^{\gamma}$	0.19 (± 0.05)	2.34 (± 0.10)	0.10 (± 0.05)

SE, standard error; ns, not statistically significant

All the models, either independently or simultaneously fitted, were found to provide non-significant bias (Table 7). The simultaneously predicted crown biomass and AGB were strongly more correlated to observed crown biomass, and AGB, respectively, than the independently predicted ones (Table 8). Simultaneously predicted crown biomass, and AGB were 9 and 4% more correlated to relevant observed biomasses than the independently predicted ones.

Table 9 shows the tree component C stocks estimated based on NSUR models, C stocks in necromass and the SOC stock. The overall C stock was estimated at approximately 48 Mg ha^{-1}, of which 90% (43 Mg ha^{-1}) was from the soil, 9.6% from live AGB, and 0.50% (0.22 Mg ha^{-1}) from

Table 4 Fit statistics and predictive ability of independently fitted allometric biomass models

Tree component	Model form	AIC	FI	CVr [%]	Mr [%]	MPE
Stem	$\hat{Y} = \alpha RCD^{\beta}$	882.44	18.25	28.72	– 1.29^{ns}	3.26
	$\hat{Y} = \alpha RCD^{\beta}H^{\gamma}$	884.41	18.25	28.72	– 1.27^{ns}	3.37
Foliage	$\hat{Y} = \alpha RCD^{\beta}$	111.27	0.94	24.49	– 3.54^{ns}	0.59
	$\hat{Y} = \alpha RCD^{\beta}H^{\gamma}$	108.34	0.93	23.90	– 3.46^{ns}	0.61
	$Y = \alpha RCD^{\beta}LCL^{\gamma}$	112.64	0.94	24.42	– 3.66^{ns}	0.60
	$\hat{Y} = \alpha RCD^{\beta}CD^{\gamma}$	111.37	0.93	24.26	– 3.66^{ns}	0.60
Branches	$\hat{Y} = \alpha RCD^{\beta}$	606.75	18.03	19.00	– 0.66^{ns}	2.27
	$\hat{Y} = \alpha RCD^{\beta}H^{\gamma}$	606.83	17.95	18.79	– 0.70^{ns}	2.31
	$\hat{Y} = \alpha RCD^{\beta}LCL^{\gamma}$	601.60	17.75	18.23	– 0.69^{ns}	2.30
	$\hat{Y} = \alpha RCD^{\beta}CD^{\gamma}$	588.52	17.24	16.86	– 1.26^{ns}	2.28
Crown	$\hat{Y} = \alpha RCD^{\beta}$	713.11	27.31	17.57	– 0.40^{ns}	2.79
	$\hat{Y} = \alpha RCD^{\beta}H^{\gamma}$	712.14	27.14	17.26	– 0.43^{ns}	2.87
	$\hat{Y} = \alpha RCD^{\beta}LCL^{\gamma}$	708.58	26.92	16.89	– 0.55^{ns}	2.85
	$\hat{Y} = \alpha RCD^{\beta}CD^{\gamma}$	699.35	26.38	15.95	– 1.01^{ns}	2.82
Shoot system	$\hat{Y} = \alpha RCD^{\beta}$	1087.92	100.76	19.91	– 1.01^{ns}	5.86
	$\hat{Y} = \alpha RCD^{\beta}H^{\gamma}$	1089.14	100.59	19.82	– 1.06^{ns}	5.90
	$\hat{Y} = \alpha RCD^{\beta}LCL^{\gamma}$	1089.85	100.74	19.90	– 1.07^{ns}	6.13
	$\hat{Y} = \alpha RCD^{\beta}CD^{\gamma}$	1086.00	99.89	19.48	– 1.36^{ns}	5.94

Table 5 Regression parameters of simultaneously fitted allometric biomass models

Tree component	Model form	α_1 (± SE)	β_1 (± SE)	α_2 (± SE)	β_2 (± SE)	γ_2 (± SE)	α_3 (± SE)	β_3 (± SE)	γ_3 (± SE)
Stem	$\hat{Y} = \alpha_1 RCD^{\beta 1}$	0.03 (± 0.01)	2.96 (± 0.09)						
Foliage	$\hat{Y} = \alpha_2 RCD^{\beta 2} H^{\gamma 2}$			0.01 (± 3E − 03)	2.48 (± 0.08)	0.13 (± 0.02)			
Branches	$\hat{Y} = \alpha_3 RCD^{\beta 3} CD^{\gamma 3}$						0.70 (± 0.11)	1.28 (± 0.07)	0.30 (± 0.04)
Crown	$\hat{Y} = \alpha_2 RCD^{\beta 2} H^{\gamma 2} + \alpha_3 RCD^{\beta 3} CD^{\gamma 3}$			0.01 (± 3E − 03)	2.48 (± 0.08)	0.13 (± 0.02)	0.70 (± 0.11)	1.28 (± 0.07)	0.30 (± 0.04)
Shoot system	$\hat{Y} = \alpha_1 RCD^{\beta 1} + \alpha_2 RCD^{\beta 2} H^{\gamma 2} + \alpha_3 RCD^{\beta 3} CD^{\gamma 3}$	0.03 (± 0.01)	2.96 (± 0.09)	0.01 (± 3E − 03)	2.48 (± 0.08)	0.13 (± 0.02)	0.70 (± 0.11)	1.28 (± 0.07)	0.30 (± 0.04)

necromass. Mean soil bulk density was 1.22 g cm^{-3} (± 0.03), mean SOC content was 1.18% (± 0.07), and the SOM content was 2.04% (± 0.13).

The C stored in live AGB was estimated at 4.56 Mg ha^{-1}, with 57 (2.6 Mg ha^{-1}), 32 (1.5 Mg ha^{-1}), and 11% (0.5 Mg ha^{-1}) allocated to stem, branches and foliage, respectively. Live stumps accounted insignificantly to live AGB. Approximately 93% (0.2 Mg ha^{-1}) of the C stored in necromass was from FWD and litter, and about 7% from CWD. The logs accounted for about 100% of the CWD.

Discussion

Non-destructive Biomass Sampling

The typical methods for measuring biomass and developing biomass models require destructive sampling of trees. Destructive biomass sampling is deemed the most accurate method (Dong et al. 2016). In this study, the dry mass of the stem and branches were determined non-destructively by multiplying their volumes by the basic density of a basal wood section of the thickest primary branch. The basic density of the basal wood section was taken as representative of the whole tree, ignoring possible within tree variations.

The stem dry mass is normally calculated destructively either as the product of stem volume and the basic density of a disc(s) removed from the main stem (Magalhães and Seifert 2015; Magalhães 2015) or as a product of fresh mass and the ratio of oven-dry- to fresh-mass of the disc(s) (Dong et al. 2016; Tran et al. 2016). The second method is also applied to the branches.

However, while Swenson and Enquist (2008) suggested that branch wood density is representative of stem wood density, they found trunks to be denser than branches. Sarmiento et al. (2011) observed that trunk xylem is denser than branch xylem and Okai et al. (2004) found otherwise. On the other hand, branches density has been reported to decrease along crown level (Dibdiakova and Vadla 2012). These factors may have led to an over- or underestimation of the stem and branch biomasses.

Because the study was conducted in a protected area, where destruction of trees is prohibited, non-destructive sampling techniques are the only available for biomass estimation. Other ground-based non-destructive biomass techniques include using (1) (imported) general biomass allometric models, (2) mean literature values of basic wood density, (3) trunk wood cores. Yet, the biomass estimates from this study are expected to be much more accurate than when using (imported) general biomass allometric models and/or mid-values of published basic wood densities of specific species as done by Stringer et al. (2015), since tree (biomass) allometry varies with the environment (Anderson-Texeira et al.

Table 6 Fit statistics and predictive ability of simultaneously fitted allometric biomass models

Tree component	Model form	AIC	FI	CVr [%]	Mr [%]	MPE
Stem	$\hat{Y} = \alpha_1 RCD^{\beta 1}$	883.43	18.33	28.98	-1.40^{ns}	3.27
Foliage	$\hat{Y} = \alpha_2 RCD^{\beta 2} H^{\gamma 2}$	106.74	0.93	24.13	-3.50^{ns}	0.60
Branches	$\hat{Y} = \alpha_3 RCD^{\beta 3} CD^{\gamma 3}$	588.81	17.31	17.05	-1.29^{ns}	2.30
Crown	$\hat{Y} = \alpha_2 RCD^{\beta 2} H^{\gamma 2} + \alpha_3 RCD^{\beta 3} CD^{\gamma 3}$	685.97	24.54	14.22	-0.22^{ns}	2.00
Shoot system	$\hat{Y} = \alpha_1 RCD^{\beta 1} + \alpha_2 RCD^{\beta 2} H^{\gamma 2} + \alpha_3 RCD^{\beta 3} CD^{\gamma 3}$	1079.03	93.91	17.48	-1.00^{ns}	4.62

2015; Siliprande et al. 2016; Sharma and Zhang 2004), tree size, species, crowding by neighbours and exposure to light and wind (King 2011). On the other hand, wood density is known to vary substantially within the stem and between trees and sites (Seifert and Seifert 2014). Thus, as maintained by these authors, "to base biomass upscaling merely on mean literature values of basic density is a very crude approach that might, due to density variations within and between trees, lead to seriously biased estimates". Using trunk wood cores (using increment borer) to estimate tree biomass is not feasible for smaller trees (e.g. with diameter < 4 cm).

Additivity

It was observed that, by using the NSUR approach, the predictive accuracy and ability of the major component models (crown and AGB models) improved significantly when compared to the same component models fitted independently. This is because the data were consistent with the restrictions and because the models fitted as well with the restriction imposed, as revealed by the *t*-test results for the restriction imposed on NSUR (*p* value ≈ 1). However, Nord-Larsen et al. (2017) observed a decline in predictive accuracy and increased model bias when using the NSUR approach to achieve additivity. On the other hand, in this study, no significant differences were observed between the simultaneously and independently fitted minor component models (stem, foliage and branches) with regard to predictive accuracy and ability. This is in line with the findings by Sanquetta et al. (2015).

When using the independently fitted models to the testing data, it was observed unexpectedly that, for trees with RCD < 3, the predicted branches biomass was larger than the predicted crown biomass, and AGB. As maintained by Parresol (2001), if one component (e.g. branches) is part of another component (e.g. crown, AGB), it is logical to expect the estimate of the part not to exceed that of the whole. This inconsistency was due to violation of the property of additivity. In fact, this inconsistency was not observed when using simultaneously fitted models (i.e. taking into consideration the property of additivity).

Carbon Stocks

The estimates of C stored in AGB (4.59 Mg ha $^{-1}$) are well below the estimates of other mangrove forests of Mozambique: in the Sofala Bay (Sitoe et al. 2014), and within

Table 7 Validation of independently and simultaneously fitted models

	Tree component	Bias [%]	*V*	p value
Independentely fitted models	$Stem_i$	– 2.11	1675	0.12
	$Foliage_i$	– 1.19	1625	0.20
	$Branches_i$	0.08	1471	0.65
	$Crown_i$	– 0.41	1427	0.83
	AGB_i	– 1.96	1376	0.95
Simultaneously fitted models	$Stem_s$	– 2.96	1609	0.23
	$Foliage_s$	– 1.77	1573	0.32
	$Branches_s$	0.45	1501	0.54
	$Crown_s$	– 0.11	1472	0.65
	AGB_s	– 1.74	1479	0.62

Subscripts i and s indicate predicted biomass using independently and simultaneously fitted models, respectively. *V* is the Wilcoxon statistic

Table 8 Person's correlation test of significance between predicted and observed biomass

Observed vs. predicted biomass	Pearson's correlation test	
	r	p value
$Stem_o \times Stem_i$	0.94	0.00
$Foliage_o \times Foliage_i$	0.94	0.00
$Branches_o \times Branches_i$	0.86	0.00
$Crown_o \times Crown_i$	0.90	0.00
$AGB_o \times AGB_i$	0.94	0.00
$Stem_o \times Stem_s$	0.94	0.00
$Foliage_o \times Foliage_s$	0.94	0.00
$Branches_o \times Branches_s$	0.86	0.00
$Crown_o \times Crown_s$	0.98	0.00
$AGB_o \times AGB_s$	0.97	0.00

Subscripts i and s indicate predicted biomass using independently and simultaneously fitted models, respectively; and subscript o indicate observed biomass

Table 9 Mean C stocks [Mg ha $^{-1}$] (± SE) of each biomass and necromass component

Live biomass						
Stem	Foliage	Branches	Crown	AGB	Live stumps	Total
2.63 (± 0.34)	0.49 (± 0.06)	1.47 (± 0.14)	1.96 (± 0.20)	4.59 (± 0.53)	4E – 07 (± 4E – 08)	4.59 (± 0.53)
Necromass and SOC						
Snags	Dead stumps	Logs	CWD	FWD + Litter	Total	SOC
2E – 06 (± 2E – 07)	6E – 06 (± 3E – 07)	0.01 (± 2E – 03)	0.01 (± 2E – 03)	0.20 (± 7E – 03)	0.22 (± 0.06)	43.08 (± 2.49)

the Zambezi River Delta (Stringer et al. 2015). The estimates by Sitoe et al. (2014) (28.02 Mg ha $^{-1}$) are 6-fold higher than those from this study; and the estimates by Stringer et al. (2015) (≈ 147 Mg ha $^{-1}$) are 32-fold higher than the current estimates. The C stocks in AGB of this study are lower because are from a juvenile secondary mangrove forest composed mainly by seedlings and samplings, where more than 85% of the trees had RCD ≤ 10 cm and heights ≤2 m. However, the study areas by Sitoe et al. (2014) and Stringer et al. (2015) are composed by old primary mangroves, with DBH up to 45 cm, and canopy height up to 29 m, respectively.

Carbon stored in CWD of this study is considerably smaller than that reported by Meriem et al. (2016) (diameters >10 cm), Adame et al. (2013) (diameters >2.5 cm), Sitoe et al. (2014) for mangrove forests. This is so because the study area is located in a peri-urban area of Maputo city, where approximately 74% of the population rely on wood fuel to meet its energy needs (Bouwer and Falcão 2004). Thus CWD are collected and used as firewood by the local community, as collecting wood debris is not prohibited by the municipality; whereas, most mangrove forests are mainly located in remote areas (Stringer et al. 2015), where there is no shortage of firewood, and thus little pressure for CDW. In fact, it was noted in this study that 93% of C stored in necromass was from FWD and litter; CDW accounted with only 7%.

Soil bulk density, SOC content, and SOM content of the surface soil (0–30 cm) of the current study were in line with those by Sitoe et al. (2014), Stringer et al. (2015), and Kristensen et al. (2008). SOC stock accounted for 90% of ecosystem C stock; this is in accordance with the percentage of mangrove ecosystem C stock allocated to soils reported by Adame et al. (2013) (78–99%), Nam et al. (2016) (90.5%), Sitoe et al. (2014) (73.28%), Donato et al. (2011) (71–98%), Kauffman et al. (2011) (70%). However, the SOC stock of this study is likely to be underestimated because it was based on the surface soil (0–30 cm) only, whereas several studies have reported that organic-rich soils may extend up to several meters (Donato et al. 2011; Kauffman et al. 2011).

The insignificant amount of C stocks in live and dead stumps reveals that the conservation status of the mangroves of western cost of Maputo city is satisfactory, as it reveals the low intensity of anthropogenic disturbances.

Conclusion

This study was aimed to fit tree component and aboveground biomass models and estimate the C stored in biomass, necromass and in the soil of a juvenile secondary Mangrove forest, composed mainly by seedlings and saplings. Besides the advantage of enforcing the property of additivity, the models fitted simultaneously using NSUR approach were, overall, superior in terms of predictive accuracy and ability compared to those fitted independently. The developed biomass models are a significant contribution to the available published models, especially for juvenile mangrove trees (seedling and sapling) which are lacking in the literature and yet required for increasing of young successional mangrove forests as result of disturbances. The ecosystem C stock was estimated at 48 Mg ha^{-1}, of which 90% was from the surface soil, 9.6% from live AGB, and 0.50% from necromass. Of the C stored in live AGB (4.56 Mg ha^{-1}), 57, 32, and 11% were allocated to stem, branches, and foliage, respectively; and 93% of C stored in necromass was from FWD and litter.

Acknowledgements Thanks are addressed to the field team and to the anonymous reviewers.

Compliance with Ethical Standards

Conflict of Interest There is no conflict of interest.

References

Adame MF, Kauffman JB, Medina I et al (2013) Carbon stocks of tropical coastal wetlands within the karstic landscape of the Mexican Caribbean. PLoS One 8(2):e56569. https://doi.org/10.1371/journal.pone.0056569

Akaike H (1973) Information theory as an extension of the maximum likelihood principle. In: Petrov BN, Csaki F (eds.) Second international symposium on information theory. Budapest, Akademiai Kiado, pp 267–281.

Alfons A (2015) cvTools: cross-validation tools for regression models (R Package Version 0.3.2). R Foundation for Statistical Computing, Vienna

Amade FMZ (2006) Estudo da Estrutura de três Comunidades de Mangal (A.marina, C.tagal e R.mucronata) em três locais na Baía de Maputo, Costa do Sol, Ponta Rasa e Saco da Inhaca. B.Sc. Thesis, UEM, Maputo.

Anderson-Texeira KJ, McGarvey JC, Muller-Landau HC et al (2015) Size-related scaling of tree form and function in a mixed-age forest. Functional Ecology 29:1587–1602. https://doi.org/10.1111/1365-2435.12470

Annighöfer P, Ameztegui A, Ammer C et al (2016) Species-specific and generic biomass equations for seedlings and saplings of European tree species. European Journal of Forest Research 135:313–329. https://doi.org/10.1007/s10342-016-0937-z

Baccini A, Goetz SJ, Walker WS et al (2012) Estimated carbon dioxide emissions from tropical deforestation improved by carbon-density maps. Nature Climate Change 2:182–185

Barbosa FMA, Cuambe CC, Bandeira SO (2001) Status and distribution of mangroves in Mozambique. South African Journal of Botany 67: 393–398

Bolte A, Rahmann T, Kuhr M et al (2004) Relationships between tree dimension and coarse root biomass in mixed stands of European beech (Fagus sylvatica L.) and Norway spruce (*Picea abies* [L.] Karst.). Plant and Soil 264:1–11

Bouwer R, Falcão MP (2004) Wood fuel consumption in Maputo, Mozambique. Biomass and Bioenergy 27:233–245

Brasil MAM, Veiga RAA, Timoni JL (1994) Erros na determinação da densidade básica da madeira. CERNE 1(1):55–57

Bunster J (2006) Commercial timbers of Mozambique. Technological catalogue. Traforest Lda, Maputo.

Chao KJ, Philips OL, Baker TR (2008) Wood density and stocks of coarse woody debris in a northwestern Amazonian landscape. Canadian Journal of Forest Research 38:795–805

CMM (2010) Perfil estatístico do município de Maputo. Conselho Municipal de Maputo, Maputo

de Gier IA (1992) Forest mensuration (fundamentals). ITC, The Netherlands

de Jong TJ, Klinkhamer PGI (2005) Evolutionary ecology of plant reproductive strategies. Cambridge University Press, New York

Dibdiakova J, Vadla K (2012) Basic density and moisture content of coniferous branches and wood in Northern Norway. EPJ Web of Conferences 33. https://doi.org/10.1051/epjconf20123/302005.

DINAGECA (1997) Mapa digital de uso e cobertura de terra. Cenacarta, Maputo

Donato DC, Kauffman JB, Murdiyarso D et al (2011) Mangroves among the most carbon-rich forests in the tropics. Nature Geoscience 4: 293–297

Dong L, Zhang L, Li F (2016) Developing two additive biomass equations for three coniferous plantation species in Northeast China. Forests 7(136):1–21

Elias M, Potvin C (2003) Assessing inter- and intra-specific variation in trunk carbon concentration for 32 Neotropical tree species. Canadian Journal of Forest Research 33:1039–1045

FAO (2003) FAO map of world soil resources. Rome, Food and Agriculture Organisation of the United Nations, Rome

FAO (2007) The World's mangroves 1980 – 2005. FAO Forestry Paper 153.

Fatoyinbo TE, Simard M, Washington-Allen RA et al (2008) Landscape-scale extent, height, biomass, and carbon estimation of Mozambique's mangrove forests with Landsat ETM+ and shuttle radar topography Mission elevation data. Journal of Geophysical Research 113:1–13

Furnival GM (1961) An index for comparing equations used in constructing volume tables. Forest Science 7:337–341

Galik CS, Mobley ML, Richter D (2009) A virtual "field test" of forest management carbon offset protocols: the influence of accounting. Mitigation and Adaptation Strategies for Global Change 14:677–690

Geri C, Ochieng E, Tieszen LL et al (2011) Status and distribution of mangrove forests of the world using earth observation satellite data. Global Ecology and Biogeography 20:154–159

Hamilton SE, Lovette J (2015) Ecuador's mangrove forest carbon stocks: a spatiotemporal analysis of living carbon holdings and their depletion since the advent of commercial aquaculture. PLoS One 10(3): e0118880. https://doi.org/10.1371/journal.pone.0118880

Harmon M, Hua C (1991) Coarse wood debris dynamics in two old-growth ecosystems: comparing a deciduous forest in China and a conifer forest in Oregon. BioScience 41(9):604–610

Harmon ME, Franklin JF, Swanson FJ et al (1986) Ecology of coarse woody debris in temperate ecosystems. Advances in Ecological Research 15

Hoguane AM (2007) Perfil diagnóstico da zona costeira de Moçambique. Revista de Gestão Costeira Integrada 7(1):69–82

Husch B, Beers TW, Kershaw JA Jr (2003) Forest mensuration, 4th edn. John Willey & Sons, New York

IPCC (2003) Good Practice Guidance for Land Use, Land-Use Change and Forestry. In: Penman J, Gytarsky M, Hiraishi T et al (eds) Intergovernmental Panel on Climate Change. IGES, Hayama

IPCC (2006) Guidelines for national greenhouse gas inventories. In: Eggleston S, Buendia L, Miwa K et al (eds) Agriculture, Forestry and Other Land Use, vol 4. IGES, Hayama

Jachowski NRA, Quak MSY, Friess DA et al (2013) Mangrove biomass estimation in Southwest Thailand using machine learning. Applied Geography 45:311–321

Kauffman JB, Helder C, Cole TG et al (2011) Ecosystem carbon stocks of Micronesian mangrove forests. Wetlands 31:343–352

King DA (2011) Size-related changes in tree proportions and their potential influence on the course of height growth. In: Meinzer FC, Lachenbruch B, Dawson TE (eds) Size- and age-related changes in tree structure and function. Springer, New York, pp 165–192

Kristensen E, Bouillon S, Dittmar T et al (2008) Organic carbon dynamics in mangrove ecosystems: a review. Aquatic Botany 89:201–219

Ladd B, Laffan SW, Amelung W et al (2012) Estimates of soil carbon concentration in tropical and temperate forest and woodland from available GIS data on three continents. Global Ecology and Biogeography 22:461–469. https://doi.org/10.1111/j.1466-8238.2012.00799.x

Magalhães TM (2015) Allometric equations for estimating belowground biomass of Androstachys johnsonii Prain. Carbon Balance and Management 10:16

Magalhães TM, Seifert T (2015) Tree component biomass expansion factors and root-to-shoot ratio of Lebombo ironwood: measurement uncertainty. Carbon Balance and Management 10:9

Merganičová K, Merganič J (2010) Coarse woody debris carbon stocks in natural spruce forests of Babia hora. Journal of Forest Science 56(9): 397–405

Meriem S, Tjitrosoedirjo S, Kotowska MM et al (2016) Carbon and nitrogen stocks in dead wood of tropical lowland forests as dependent on wood decay stages and land-use intensity. Annals of Forest Research 59(2):299–310

Nam VM, Sasmito SD, Murdiyarso D et al (2016) Carbon stocks in artificially and naturally regenerated mangrove ecosystems in the Mekong Delta. Wetlands Ecology and Management 24:231–244

Nord-Larsen T, Meilby H, Skovsgaard JP (2017) Simultaneous estimation of biomass models for 13 tree species: effects of compatible additivity requirements. Canadian Journal of Forest Research 47: 765–776. https://doi.org/10.1139/cjfr-2016-0430

Okai R, Frimpong-Mensah K, Yeboah D (2004) Characterization of strength properties of branchwood and stemwood of some tropical hardwood species. Wood Science and Technology 38:163–171

Pan Y, Birdsey RA, Fang J et al (2011) A large and persistent carbon sink in the World's forests. Science 133:988–993

Parresol B (2001) Additivity of nonlinear biomass equations. Canadian Journal of Forest Research 31:865–878

Pearson T, Walker SM, Brown S (2005) Sourcebook for land use, land-use change and forestry projects. Winrock International, Washington DC

R Core Team (2016) A language and environment for statistical computing. R Foundation for Statistical Computing, Vienna

Salis SM, Assis MA, Mattos PP et al (2006) Estimating the aboveground biomass and wood volume of savannah woodlands in Brazil's Pantanal wetlands based on allometric correlations. Forest Ecology Management 228:61–68

Sanquetta CR, Behling A, Corte APD et al (2015) Simultaneous estimation as alternative to independent modeling of tree biomass. Annals of Forest Science 72:1099–1112

Sarmiento C, Patiño S, Paine CET et al (2011) Within-individual variation of trunk and branch xylem density in tropical trees. American Journal of Botany 98(1):140–149

SAS Institute Inc. (1999) SAS/ETS User's Guide, Version 8. SAS Institute Inc., Cary

Schroeder P, Brown S, Mo J et al (1997) Biomass estimation for temperate broadleaf forest of the United States using inventory data. Forest Science 43:424–434

Seifert T, Seifert S (2014) Modelling and simulation of tree biomass. In: Seifert T (ed) Bioenergy from wood: sustainable production in the tropics. Springer, New York, pp 43–66

Sharma M, Zhang SY (2004) Height–diameter models using stand characteristics for *Pinus banksiana* and *Picea mariana*. Scandinavian Journal of Forest Research 19:442–451

Siliprande NC, Nogueira EM, Toledo JJ et al (2016) Inter-site variation in allometry and wood density of *Goupia glabra* Aubl. in Amazonia. Brazilian Journal of Biology. https://doi.org/10.1590/1519-6984.22514.

Sitoe AA, Mondlate LJC, Guedes BS (2014) Biomass and carbon stocks of Sofala bay mangrove forests. Forests 5:1967–1981

Spiess A, Neumeyer N (2010) An evaluation of R as an inadequate measure for nonlinear models in pharmacological and biochemical research: a Monte Carlo approach. BMC Pharmacology 10:6

Stringer CE, Trettin CC, Zarnoch CJ, Tang W (2015) Carbon stocks of mangroves within the Zambezi River Delta, Mozambique. Forest Ecology and Management 354:139–148

Swenson NG, Enquist BJ (2008) The relationship between stem and branch wood specific gravity and the ability of each measure to predict leaf area. American Journal of Botany 95(4):516–519

Taylor M, Ravilious C, Green EP (2003) Mangroves of East Africa. UNEP-WCMC, Cambridge

Ter-Mikaelian MT, Korzukhin MD (1997) Biomass equation for sixty five north American tree species. Forest Ecology and Management 97:1–27

Tran P, Gritcan I, Cusens J et al (2016) Biomass and nutrient composition of temperate mangroves (Avicennia marina var. australasica) in New Zealand. New Zealand Journal of Marine and Freshwater Research 51:427–442. https://doi.org/10.1080/00288330.2016.1260604

Zarin DJ (2012) Carbon from tropical deforestation. Science 336:1518–1519

Zhou ZY, Osbert J, Huang JH et al (2007) Soil carbon and nitrogen stores and storage potentials affected by land-use in an agro-pastoral ecotone of northern China. Biogeochemistry 82:127–138